Li *et al. Biology Direct* (2025) 20:23
https://doi.org/10.1186/s13062-025-00617-y

Biology Direct

RESEARCH

Open Access

Sigma-1 receptor activation attenuates DOX-induced cardiotoxicity by alleviating endoplasmic reticulum stress and mitochondrial calcium overload via PERK and IP3R-VDAC1-MCU signaling pathways

Zixuan Li[1,2,3†], Qian Ran[4†], Chuan Qu[1,2,3†], Shan Hu[1,2,3], Shengyu Cui[1,2,3], You Zhou[1,2,3], Bo Shen[1,2,3*] and Bo Yang[1,2,3*]

Abstract

Background Doxorubicin (DOX) is an anthracycline with potent antitumor properties and rare yet serious cardiotoxic side effects that limit its clinical application. The sigma-1 receptor is a stress-triggered chaperone often dysregulated in diseases and has known cardioprotective effects. Although its anti-oxidative stress and anti-apoptotic effects have been demonstrated, its effectiveness in DOX-induced cardiotoxicity has never been explored. This study investigated the potential role of the activated sigma-1 receptor in a DOX-induced murine cardiotoxicity model to elucidate the receptor's mechanism of action.

Methods We established the model in C57BL/6 mice by daily intraperitoneal injections of fluvoxamine (Flv) for 4 consecutive weeks to activate the receptor and by weekly intraperitoneal injections of DOX at 5 mg/kg for 3 weeks. We performed in vitro experiments using cardiomyocytes of neonatal Sprague–Dawley rats to verify the protective effect of the sigma-1 receptor.

Results We found that sigma-1 expression in the heart decreased in the DOX-treated mice, and activating the receptor with Flv improved cardiac function. Moreover, Flv pretreatment inhibited cardiomyocyte apoptosis and endoplasmic reticulum stress and increased the expression of the Bcl2 apoptosis regulator (Bcl2), effectively alleviating the pathophysiological manifestations in mice. In addition, activating the receptor exerted cardioprotective effects by modulating endoplasmic reticulum stress through the PRKR-like endoplasmic reticulum kinase (PERK) signaling pathway. It also reduced mitochondrial and endoplasmic reticulum contact and alleviated mitochondrial calcium overload through the IP3R-VDAC1-MCU signaling pathway.

†Zixuan Li, Qian Ran and Chuan Qu have contributed equally to the manuscript.

*Correspondence:
Bo Shen
shenbowhdx@126.com
Bo Yang
yybb112@whu.edu.cn
Full list of author information is available at the end of the article

Conclusion In conclusion, our study emphasizes the therapeutic potential of activating sigma-1 receptors against DOX-induced cardiotoxicity, suggesting sigma-1 receptors as potential therapeutic targets for this disease.

Keywords Sigma-1 receptor, DOX-induced cardiotoxicity, MAM, ER stress, Ca^{2+} overload, PERK signaling pathway, IP3R-VDAC1-MCU signaling pathway

Introduction

Doxorubicin (DOX) is a representative broad-spectrum anthracycline-based chemotherapeutic agent widely used in treating various solid tumors, such as breast and ovarian tumors and hematological malignant tumors [1]. Although it exerts considerable anticancer effects, its clinical benefit is limited by dose-dependent cardiotoxicity, including acute and chronic cardiac injury, arrhythmias, hypotension, refractory delayed cardiomyopathy, and even heart failure [2]. Evidence shows that the correlation between cumulative DOX doses of 400 mg/m^2 and 500 mg/m^2 and heart failure is 5% and 16%, respectively, and the accumulated DOX doses of 550 mg/m^2 sharply increase this correlation to 26% [3]. Many mechanisms of DOX-induced cardiotoxicity have been widely demonstrated and include causing apoptosis, endoplasmic reticulum (ER) stress, mitochondrial oxidative stress, mitochondrial autophagy, organelle damage, and dysregulation of calcium homeostasis [4, 5]. However, to date, no effective targeted therapeutic strategy exists to prevent or eliminate DOX-triggered cardiotoxicity in clinical settings, imposing a heavy global socioeconomic and medical burden. Therefore, understanding the molecular mechanisms underlying DOX-induced cardiotoxicity is crucial for developing preventive measures against it.

Endoplasmic reticulum (ER) stress and dysregulation of calcium homeostasis have been proposed as the mechanisms of DOX-induced cardiotoxicity [6]. In cells, the ER is a vital intracellular storage reservoir in contact with mitochondria that forms a complex meshwork called the mitochondria-associated endoplasmic reticulum membrane (MAM) [7]. This entangled network builds up a natural channel for calcium transport between the mitochondria and the ER [8]. Ca^{2+} is an essential second messenger for intracellular signaling and electrical activity in the heart and directly activates myocardial contractions [9]. Therefore, calcium homeostasis is pivotal for maintaining cell survival and normal diastolic function of the heart. As the heart beats, a steady stream of Ca^{2+} is released from the ER and channeled through the MAM into the cytoplasm and mitochondria, mediating muscle contractions [10]. When the body is subjected to external stimuli, ER stress occurs, inducing a chain of events that provoke cell damage and apoptosis in the heart. Specifically, the stimuli may promote the expression and accumulation of misfolded and unfolded proteins that trigger ER stress, hindering its function and driving conformational changes in the MAM [11]. Consequently, the abnormal calcium signaling promotes Ca^{2+} accumulation in mitochondria, impairing the respiratory chain and mitochondrial bioenergetic homeostasis and triggering apoptosis [12]. Thus, the MAM network ensures the contact between the ER and mitochondria and has a crucial regulatory role in disease development.

Sigma-1 receptors are ligand-controlled chaperone proteins with cardioprotective effects [13]. Initially, they were considered opioid receptors, distributed only in the central nervous system and closely associated with various neurodegenerative diseases. When the sigma-1 receptor was cloned, it was recognized as a non-opioid receptor with a broad distribution in peripheral organs, such as the heart, liver, and kidneys, and associated with various organic diseases [14]. The sigma-1 receptor is a transmembrane protein located in the ER membrane and mediates the signaling crosstalk between the ER and mitochondria [15]. It stabilizes the ER structure and regulates ion channels, lipid distribution, and neurotransmitter release. Under normal conditions, the sigma-1 receptor forms a complex in the ER membrane with the glucose-regulated protein, 78 kDa (GRP78/BiP) chaperone attached to the luminal side of the inositol trisphosphate (IP3) receptor [16]. When ER stress occurs, the sigma-1 receptor dissociates from GRP78 to stabilize the structure and function of the IP3 receptor, an efficient regulator of interorganelle signaling [7]. After an extensive literature search, we found that fluvoxamine (Flv) is a potent sigma-1 receptor inducer that effectively activates the sigma-1 receptor [17]. Activating the sigma-1 receptor reduces the contact between mitochondria and the ER, relieving ER and mitochondrial oxidative stress, alleviating mitochondrial calcium overload, upregulating the expression of the Bcl2 apoptosis regulator (Bcl2), and attenuating myocardial injury [18]. Because the role of the sigma-1 receptor in DOX-induced cardiotoxicity remains unclear, we sought to delineate its mechanism of action during DOX-induced myocardial damage. We hypothesized that the sigma-1 receptor alleviates ER stress and mitochondrial calcium overload to mitigate DOX-induced cardiotoxicity. Therefore, We hypothesized that the sigma-1 receptor alleviates ER stress and mitochondrial calcium overload to mitigate DOX-induced cardiotoxicity. Therefore, we established a

DOX-induced cardiotoxicity model in mice using Flv and DOX to elucidate the sigma-1 receptor's mechanism of action. We validated our model with in vitro experiments using rat cardiomyocytes.

Material and methods

Animals and treatments

Male C57BL/6 mice (8 weeks old, 20–22 g) were obtained from the Center of Experimental Animals, China Three Gorges University, and were housed in a temperature-controlled room (20 ± 5 °C) with a 12–12 h dark–light cycle and free access to water and food. All animal procedures were per the institutional guidelines for the care and use of laboratory animals and approved by the Animal Ethics Committee of Wuhan Myhalic Biotechnology (HLK-20231007-001). All animals were acclimatized and fed in the laboratory for 1 week before the start of the experiment.

We calculated the sample size based on our preliminary study. To detect the differences in heart function among mice given different stimuli with a two-sided 5% significance level and a power of 85%, a sample size of 10 mice per group was necessary. Mice were randomly assigned into 4 groups (n = 10): (1) control (CTL, saline); (2) doxorubicin (DOX); (3) doxorubicin + fluvoxamine (DOX + Flv); and (4) doxorubicin + fluvoxamine + BD1047 (DOX + Flv + BD). The DOX group was intraperitoneally injected with DOX at 5 mg/kg/week for 3 weeks [19, 20], and the CTL group was given an equivalent amount of saline (5 mg/kg/week). Before DOX administration, the DOX + Flv group was given daily intraperitoneal injections of Flv at 1 mg/kg/d for 4 weeks [21, 22], and the DOX + Flv + BD group was administered BD1047 at 1 mg/kg/d [23] and Flv at 1 mg/kg/d. The DOX, Flv, and BD1047 doses were replicated from previous studies.

Cell culture and chemical treatments

Sprague–Dawley rats within 3 days of neonatal age were decapitated, and their hearts were immediately collected into Petri dishes containing pre-cooled phosphate-buffered saline (PBS). Left ventricular myocardial tissue was taken and finely chopped into small pieces of 6 mm or less in diameter. The tissue was digested with 0.08% type II collagenase (Sigma-Aldrich, USA) and 0.125% protease (Sigma-Aldrich, USA) in ADS buffer: 120 mM NaCl, 20 mM $C_8H_{18}N_2O_4S$ (HEPES, pH 7.4), 8 mM NaH_2PO_4, 6 mM dextrose, 5 mM KCl, and 0.8 mM MgSO4, for 20 min in a water bath set at 37 °C. The supernatant was discarded, and the precipitate containing the cells was collected. Digestion and cell collection steps were repeated until the heart tissue was completely digested. Cardiomyocytes were isolated from fibroblasts by density gradient centrifugation with Percoll (GE Healthcare, USA) and cultured for 24 h in high-glucose Dulbecco's Modified Essential Medium (DMEM, HyClone, USA) containing 10% fetal bovine serum and 1% penicillin–streptomycin. For DOX-associated injury induction, cells were starved overnight in DMEM containing 0.5% fetal bovine serum. Subsequently, 1 μM/L DOX [24] was added to the medium, and cells were incubated for 24 h for relevant indexes. Before DOX administration, we pretreated cells for 24 h using 5 μM Flv [25], 5 μM BAPTA-AM [26–28], 5 μM Flv + siRNA-S1R, 5 μM Flv + 5 μM BD1047, or 5 μM BAPTA-AM + 5 μM BD1047 [29]. Sigma1 receptor small interfering (si) RNA and control RNA were purchased from GenePharma (Shanghai, China) and were transfected using Lipo-6000 reagent as per the manufacturer's instructions. The sequence of siRNA-S1R was: sense: 5′-ACACGTGGATGGTGGAGT A-3′; antisense: 5′-TACTCCACCATCCACGTGT-3′.

Echocardiographic measurements

Mice were anesthetized with 1.5% isoflurane gas, chest fur was shaved, and cardiac function indices were measured by transthoracic echocardiography using a VINNO 6 ultrasound Doppler imaging system (Vinno Inc., China). Left ventricular ejection fraction (LVEF), left ventricular fractional shortening (LVFS), left ventricular internal diameter at the end of systole (LVIDs), and left ventricular internal diameter at the end of diastole (LVIDd) were recorded continuously for at least 3 cycles for data analysis.

Hematoxylin–eosin and Masson's trichrome staining

Mice were sacrificed using overdose anesthesia. Their hearts were rapidly collected into a 4% paraformaldehyde solution and fixed for more than 24 h. The fixed hearts were paraffin-embedded and cut into 4-μm thick sections, followed by hematoxylin–eosin (HE) and Masson's trichrome staining to observe myocardial morphology. The fibrotic area was assessed by Image J software.

TUNEL (terminal deoxynucleotidyl transferase dUTP nick end labeling)

The TUNEL assay was performed on mouse heart sections using a TUNEL immunofluorescence kit (#11684817910; Roche, Basel, Switzerland). In the last step, the images were taken under a fluorescent microscope, and the apoptosis rate of cardiomyocytes was determined with ImageJ version 1.53.

Oxidative stress detection

Reactive oxygen species (ROS) generation was assessed using dihydroethidium (DHE) staining in vivo and dichloro-dihydro-fluorescein diacetate (DCFH-DA)

staining in vivo and in vitro. In brief, fresh frozen slices of the heart or cardiomyocytes were subjected to DHE or DCFH-DA staining at 37 °C in darkness, followed by a fluorescence microscopy analysis. Cells were treated with a 5 mM Mito-SOX solution for 15 min and visualized with an immunofluorescence microscope system (NIKON, Japan) to measure the amount of ROS produced by the mitochondria.

Immunofluorescence staining

Expression levels of the corresponding indicators in myocardial tissue were determined by immunofluorescence staining. Sections were de-paraffinized by xylene and rehydrated with different ethanol gradients. Antigen repair was done by heating the sections, and endogenous peroxidase was blocked by incubating the sections with a 3% hydrogen peroxide solution. Sections were probed with primary antibodies against the following proteins: sigma 1 (DF7363; Affinity), IP3R (A4436; ABclonal), or cTnT (ab10214; Abcam), and incubated with the corresponding secondary antibodies.

For cardiomyocyte immunofluorescence, cells were dyed with live-cell ER-Tracker Red dye (C1041S; Beyotime Biotechnology, China) to label the endoplasmic reticulum and fixed with 4% paraformaldehyde. Cells were probed with primary antibodies against IP3R (A4436; ABclonal), S1R, or cTnT, and immunofluorescence enhancement was performed with a tyramide signal amplification (TSA) reagent. The procedure was the same as that of the previous fluorescence staining. Cell nuclei were stained using DAPI. Images of each sample were randomly taken using an Olympus DX51 fluorescence microscope (Tokyo, Japan).

Transmission electron microscopy (TEM)

For in vivo experiments, cells were prefixed in 2.5% glutaraldehyde in PBS overnight and fixed with 1% buffered osmium tetroxide for 2 h at 4 °C. Graded ethanol was used to dehydrate the specimens, followed by 2 additional 15-min rinses with 100% ethanol. After being implanted, the specimens were collected, sectioned into ultrathin slices, and doubly stained with lead citrate and uranyl acetate. Slices were examined using a Tecnai G2 20 TWIN transmission electron microscope (FEI, USA).

For neonatal rat cardiomyocytes (NRCMs), cells were fixed for 1 h at 4 °C in 4% glutaraldehyde with 0.1 mM cacodylate buffer and for 1 additional hour at room temperature in 1% osmium tetroxide in the same buffer. The fixed samples were dehydrated using a graded ethanol series and embedded in Epon (an epoxy resin). Lead citrate and 2% uranyl acetate were used to stain the ultrathin slices. The slices were observed with a Hitachi H-7500 transmission electron microscope (Hitachi, Japan) to obtain TEM images. The distance between mitochondria and endoplasmic reticulum in each group was continuously measured using ImageJ, and the minimum value was included in the results for analysis.

Flow cytometry

Apoptosis was quantitatively assessed by flow cytometry using a commercial apoptosis detection kit (BD Pharmingen, USA). NRCMs were stained with 5 μl of 7-aminoactinomycin D (7-AAD) and annexin V-allophycocyanin (APC) dyes in darkness for 10 min at room temperature. Finally, the dyed cells were examined with flow cytometry (Bio-Rad Laboratories, Inc.), with early and late apoptotic cells considered apoptotic.

Acridine orange (AO) staining

Cell apoptosis was detected using the acridine orange staining kit (C0233S; Beyotime Biotechnology, China). Cells were exposed to the appropriate drug-supplemented media for 24 h, washed 3× with PBS, and stained with 200 μg/ml acridine orange for 3 min. Morphological features of apoptosis (cell shrinkage, chromatin condensation, and fragmentation) were monitored by fluorescence microscopy. The percentage of apoptotic cardiomyocytes was calculated at 20× magnification in 10 randomly selected fields on each slide.

Measurement of mitochondrial membrane potential (MMP)

Cellular MMP was determined with the JC-1 reagent (C2005; Beyotime Biotechnology, China). Per the manufacturer's instructions, cells were treated with a JC-1-containing solution for 30 min at 37 °C. The nucleus was enhanced using a DAPI solution (Sigma, USA). Finally, variations in JC-1 fluorescence were observed and documented using a fluorescence microscope.

Intracellular Ca^{2+} measurement

Use the Rhod-2/AM Fluorescent Probe Kit (S1062S; Beyotime Biotechnology, China) to detect the concentration of Ca^{2+}. First, according to the instructions to prepare a certain volume of staining solution. The culture medium was removed from the pre-cultured cells, and then the cells were rinsed three times with PBS buffer. The cells were covered with Rhod-2/AM working solution to ensure that the fluorescent probe reached a working concentration of 0.5X–2.5X. The cells were incubated at 37 °C for 10–30 min, and then the Rhod-2/AM working solution was removed. The cells were rinsed three times with buffer without probe to remove the excess or non-specific probe loaded in the mitochondria. The cells were covered with buffer, and the fluorescence intensity of the cells was observed and photographed using a

fluorescence microscope with an excitation wavelength of 552 nm and an emission wavelength of 581 nm (a black background in the field of view indicated that the excess working solution had been rinsed off). The average fluorescence intensity of the cells in the field of view was measured using ImageJ software.

Western blotting

Cardiac tissue and cell samples were harvested and lysed using RIPA lysis buffer containing a protease inhibitor and phosphatase inhibitor cocktail. Subsequently, total protein was quantified by a BCA protein assay kit. The membranes were incubated with primary antibodies: S1R (1:1000, DF7363, Affinity), Bcl2 (1:1000, A20777, ABclonal), Bax (1:1000, T40051S, AbmartIP3R (1:1000, A4436, ABclonal), BiP (1:5000, 16396-1-AP, Proteintech), PERK (1:1000, A18196, ABclonal), p-PERK (1:1000, TA4499, Abmart), eIF2α (1:500, A0764, ABclonal), p-eIF2α (1:5000, AP0692, ABclonal), ATF4 (1:1000, A0201, ABclonal), CHOP (1:1000, A20987, ABclonal), VDAC1 (1:1000, A19707, ABclonal), MCU (1:2000, A16281, ABclonal), Mfn2 (1:1000, A19678, ABclonal), Drp1 (1:5000, A21968, ABclonal), GAPDH (1:1000, GB15004, Servicebio). The membranes were incubated with HRP-conjugated secondary antibodies (1:3000, GB23303, GB23301, Servicebio). The membranes were analyzed, and Western blot images were calculated using ImageJ software.

Statistical analysis

Data were analyzed using GraphPad Prism version 8.0 and presented as mean ± standard deviation. To compare differences between multiple groups, a 1-way analysis of variance (ANOVA) was used, followed by Tukey's post hoc test. $P < 0.05$ was used as a cut-off for determining statistical significance.

Results

Activation of S1R improves myocardial contractility and attenuates myocardial fibrosis in mice

The sigma-1 receptor has high expression in the heart and exerts a cardioprotective role [13]. We examined the hearts of mice intraperitoneally injected with DOX using immunofluorescence to assess whether S1R expression relates to cardiac function. Indeed, we found that DOX administration reduced S1R receptor expression, disrupted myocardial contractile function, and worsened myocardial fibrosis.

We performed an extensive literature search and selected Flv, an S1R activator, and BD1047, an S1R inhibitor, to explore whether these 2 drugs would affect the cardiac function of healthy mice. We intraperitoneally injected the drugs into healthy mice to chronically activate the receptor and then analyzed the cardiac function of the mice. We found that LVEF, the degree of cardiac myofibril compactness, expression of the BCL2 anti-apoptotic protein, and expression of the Bax pro-apoptotic protein in mice in the injected group were unaffected compared with those in the unadministered group (Fig. 1A–D, F, H). We also performed an immunofluorescence assay and showed that S1R expression was significantly up-regulated after Flv injection but down-regulated after BD1047 injection (Fig. 1E, G). These findings indicate that the two drugs effectively activate or inhibit the S1R receptor. Moreover, we observed that neither drug affected cardiac function in healthy mice, allowing us to proceed with subsequent experiments.

We first gave the mice daily Flv, BD1047, or Flv + BD1047 injections for 4 weeks to activate or inhibit the S1R. We then administered weekly DOX injections for 3 weeks to establish a model of DOX-triggered cardiac injury and observed the changes in various aspects of the heart (Fig. 2A). After DOX treatment, the cardiac function, LVEF, and LVFS decreased significantly, while LVIDd and LVIDs increased, indicating severe damage to the heart (Fig. 2E–G). Masson's staining of the heart tissue showed that the degree of cardiac fibrosis increased significantly, and HE staining demonstrated that cardiac myofibers were arranged loosely and irregularly (Fig. 2B–D). These data suggest a successfully established mouse model of DOX-induced cardiotoxicity. Mice injected with Flv showed the opposite effect; their cardiac function improved, LVEF and LVFS increased, while LVIDd and LVIDs decreased compared with the DOX group (Fig. 2E–G). Cardiac tissue of these mice stained with HE showed that myocardial fiber arrangement was a bit more regular and denser, and myocardial collagen deposition decreased compared with that of the DOX group (Fig. 2B–D). This observation implies that Flv-induced S1R activation improves the cardiac function of the mice to a certain extent. In mice simultaneously given Flv and BD1047, the improved effects produced by S1R activation were all counteracted by the S1R inhibitor, further confirming the protective role of S1R in the DOX-induced cardiotoxicity model.

Activation of S1R inhibits cardiac oxidative stress and reduces cardiomyocyte apoptosis

First, we explored the severity of myocardial injury under different treatment conditions (Fig. 3B, F) using wheat germ agglutinin (WGA) fluorescence staining. The cardiomyocyte size was shown to have increased in response to DOX by analysis of the myocyte area via WGA staining but decreased by Flv treatment (Fig. 3A, E). Again, this protective effect of SIR on the heart was counteracted by inhibiting S1R post-activation. Next,

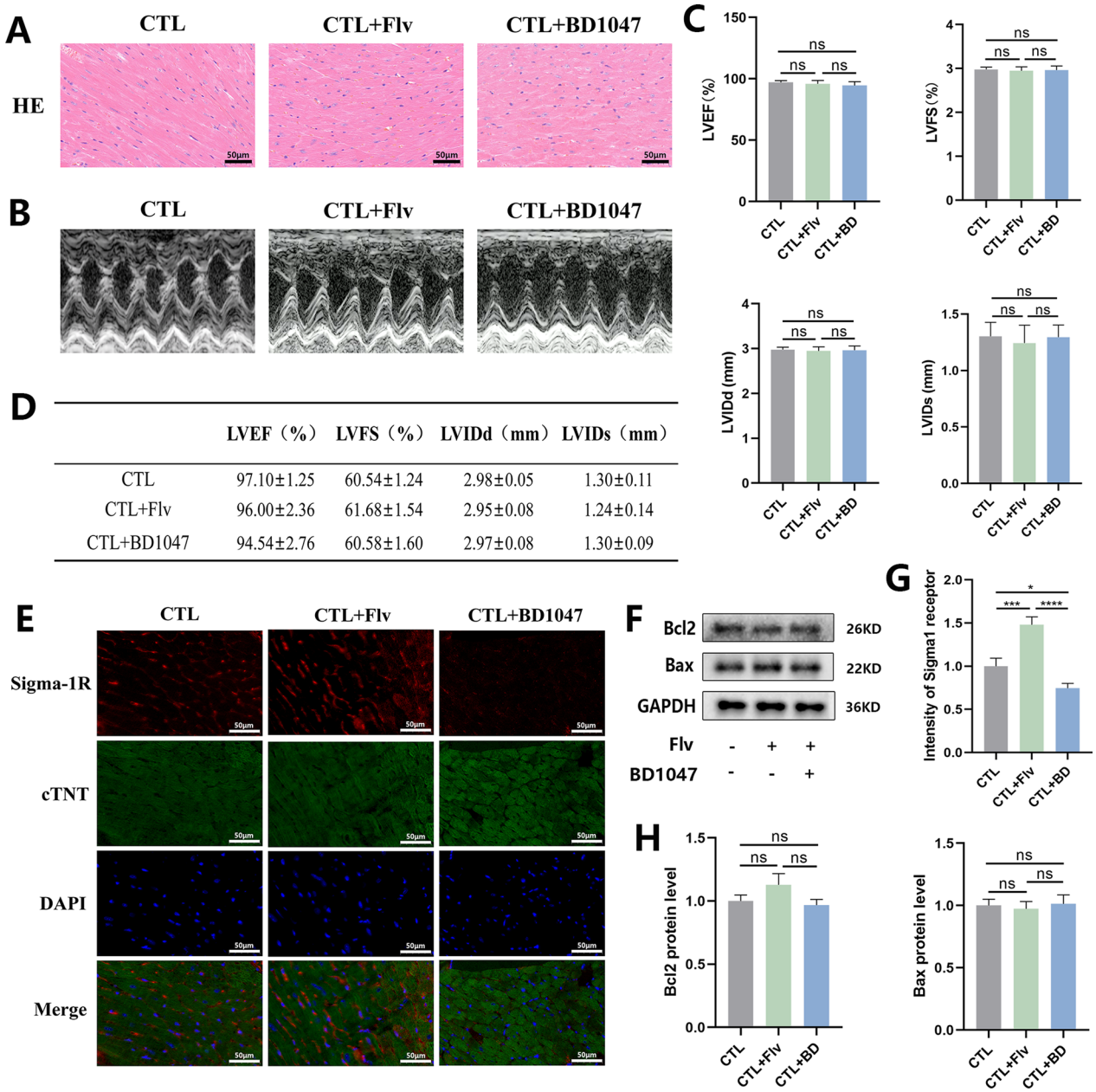

	LVEF（%）	LVFS（%）	LVIDd（mm）	LVIDs（mm）
CTL	97.10±1.25	60.54±1.24	2.98±0.05	1.30±0.11
CTL+Flv	96.00±2.36	61.68±1.54	2.95±0.08	1.24±0.14
CTL+BD1047	94.54±2.76	60.58±1.60	2.97±0.08	1.30±0.09

Fig. 1 Flv and BD1047 can effectively activate and inhibit S1R, but injection of Flv and BD1047 into normal control mice does not affect cardiac function. **A** HE staining showed that injection of Flv and BD1047 into normal mice had no effect on the arrangement of myocardial fibers. **B**–**D** Echocardiography showed no significant differences in ejection fraction and cardiac function of mice injected with Flv and BD1047 compared with normal mice (n = 3). **E** Immunofluorescence showed that S1R could be effectively activated or inhibited by Flv and BD1047 (n = 3). **F** Western blot showed that injection of Flv and BD1047 into normal mice had no significant effect on apoptosis-related proteins. **G** The statistical analysis diagrams of immunofluorescence staining reflecting S1R expression (n = 3). **H** The statistical analysis diagrams of Bcl2, Bax protein level relative to GAPDH (n = 3). *p < 0.05; ***p < 0.005; ****p < 0.001

we evaluated whether S1R affects oxidative stress in the heart during DOX-induced injury. While mice in the DOX group showed significantly elevated ROS levels, those pretreated with Flv had reduced ROS levels, suggesting S1R activation ameliorates DOX-enhanced oxidative stress (Fig. 4A, B). Cardiomyocytes from mice in the DOX group subjected to TUNEL staining showed significantly enhanced apoptosis, whereas cardiomyocytes from mice pretreated with Flv exhibited suppressed apoptosis (Fig. 3C, H). We also examined the expression

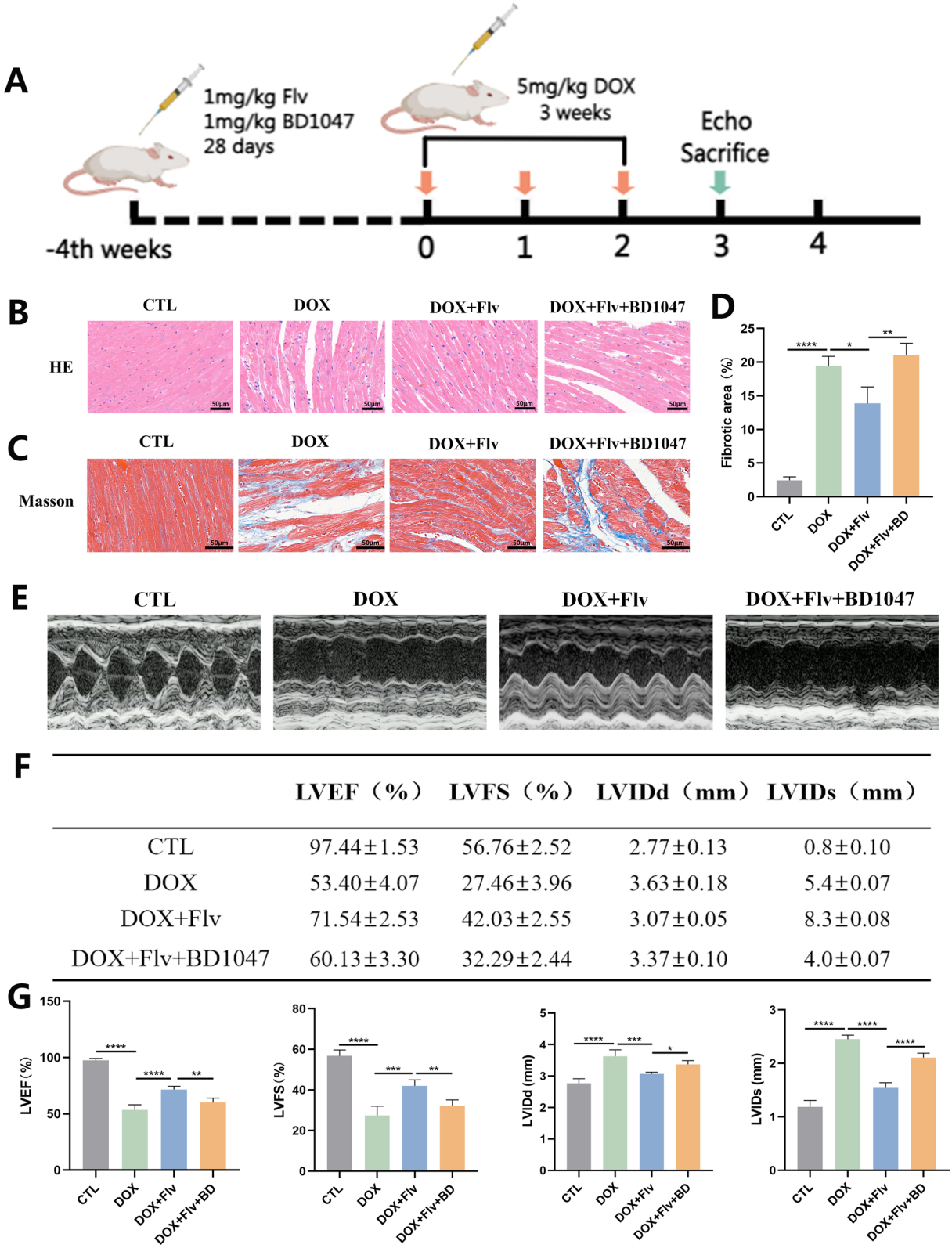

	LVEF（%）	LVFS（%）	LVIDd（mm）	LVIDs（mm）
CTL	97.44±1.53	56.76±2.52	2.77±0.13	0.8±0.10
DOX	53.40±4.07	27.46±3.96	3.63±0.18	5.4±0.07
DOX+Flv	71.54±2.53	42.03±2.55	3.07±0.05	8.3±0.08
DOX+Flv+BD1047	60.13±3.30	32.29±2.44	3.37±0.10	4.0±0.07

Fig. 2 Activation of S1R ameliorates DOX-induced cardiotoxicity and improves cardiac function. **A** Schematic protocol for Flv,BD1047 and DOX treatment. **B** HE Staining showed activation of S1R improved myocardial fiber alignment and cardiac function. **C**, **D** Masson's staining showed activation of S1R reduced myocardial fibrosis (n = 3). **E**–**G** Echocardiography showed that activation of the S1R enhanced myocardial contractility and improved cardiac function to some extent (n = 3). *p < 0.05; **p < 0.01; ***p < 0.005; ****p < 0.001

of apoptotic markers in cardiomyocytes using Western blotting. Expression of the Bcl2 anti-apoptotic protein was significantly repressed and that of the Bax pro-apoptotic protein was induced in mouse hearts after DOX treatment (Fig. 3D, G). Remarkably, this effect on the 2 apoptotic markers was reversed by Flv-induced S1R activation and counteracted by BD1047 inhibitor injections (Flv + BD1047 group).

S1R attenuates endoplasmic reticulum stress and improves mitochondrial function

So far, we demonstrated the mitigating effect of S1R on DOX-triggered cardiotoxicity in terms of animal macrophenotypes. However, microscopic manifestations in the organelles associated with the activated receptor were still unknown. Evidence shows that DOX-induced cardiotoxicity is associated with mechanisms that cause severe ER and mitochondrial oxidative stress, accompanied by mitochondrial calcium overload. Therefore, we observed mouse heart mitochondria using TEM and found that mitochondrial membranes were continuous and intact, with dense and regular cristae in healthy control mice. Conversely, after DOX injections, we observed fewer mitochondria that were also swollen and deformed with no visible cristae breaks. After Flv-induced S1R activation, the internal structure of mitochondria improved, and their function enhanced (Fig. 4C). We also examined the relevant pathways using Western immunoblotting and discovered that the ER stress pathway was significantly up-regulated in mice in the DOX group versus those in the control group. Moreover, DOX-treated mice showed increased expression of several proteins in the heart: IP3R, voltage-dependent anion channel 1 (VDAC1), mitochondrial calcium uniporter (MCU), activating transcription factor 4 (ATF4), phosphorylated eukaryotic translation initiation factor 2 alpha kinase 3 (p-PERK), and phosphorylated eukaryotic translation initiation factor 2 subunit 2 beta (p-eIF2α). In addition, DOX-treated mice had significantly elevated VDAC1-MCU calcium channel complex expression and increased mitochondrial calcium endocytosis compared with those in the control group (Fig. 4D, E). Upon S1R activation, all the above indexes decreased, ER stress weakened, and calcium circular complex expression decreased. Likewise, this mitigating effect of S1R on ER stress was opposed by adding the BD1047 inhibitor, reinforcing the protective role of S1R on the ER and mitochondria during DOX-induced cardiotoxicity.

Activation of S1R reduces ROS production and apoptosis in rat cardiomyocytes cultured in vitro

We extracted primary cardiomyocytes from rat hearts and performed in vitro experiments using rat suckling mice born 0–3 days (Fig. 5A). To more rigorously demonstrate the role of S1R, siRNA-S1R was used to knockdown S1R in some experiments. All subsequent experiments were performed by pre-treating cells with Flv, siRNA and BD1047 for 24 h. Fluorescence double labeling of S1R and cTnT proteins showed that the expression of S1R receptors in the DOX group was significantly lower than that in the control group. In contrast, Flv pretreatment increased S1R expression to a certain extent, and this effect was reversed by siRNA (Fig. 5H, J). Subsequently, we used the DCFH-DA fluorescent probe to measure the level of reactive oxygen species (ROS) in cardiomyocytes. Compared with the control group, the ROS production in the DOX group cells was significantly increased. In contrast, Flv pretreatment and subsequent S1R activation reduced the ROS level in DOX-treated cells (Fig. 5F, G). These data indicate that S1R can alleviate oxidative stress during DOX-induced cardiotoxicity, which is consistent with the results of our mouse model. We also verified this effect by quantifying protein levels through Western blotting and found that the levels of markers related to endoplasmic reticulum stress increased after DOX stimulation, but decreased after Flv-induced S1R activation (Fig. 5I, K). We also investigated whether the increase in oxidative stress levels in cardiomyocytes was associated with enhanced apoptosis by flow cytometry and Western blotting. Indeed, apoptosis of cardiomyocytes was significantly increased after DOX treatment, as indicated by a significant decrease in the expression of the anti-apoptotic protein Bcl2 and an increase in the expression of the pro-apoptotic protein Bax (Fig. 5C, E). The apoptosis rate decreased after Flv-induced S1R activation, and all indicators were relieved to a certain extent, indicating that S1R can alleviate DOX-induced oxidative stress-mediated apoptosis in vitro (Fig. 5B, D).

(See figure on next page.)

Fig. 3 Activation of S1R reduces cardiac injury and myocardial apoptosis. **A** Activation of S1R reduced cardiomyocyte size. **B** In the model of DOX-induced cardiotoxicity, S1R expression decreased. **C** TUNEL showed S1R activation attenuated cardiomyocyte apoptosis. **D** Western blot showed activation of S1R reduced cardiomyocyte apoptosis. **E** The statistical analysis diagrams of WGA reflecting cardiomyocyte size (n = 3). **F** The statistical analysis diagrams of immunofluorescence staining reflecting S1R expression (n = 3). **G** The statistical analysis diagrams of Bcl2, Bax protein level relative to GAPDH (n = 3). **H** The statistical analysis diagrams of TUNEL (n = 3). *:$p < 0.05$; **$p < 0.01$; ***$p < 0.005$; ****$p < 0.001$

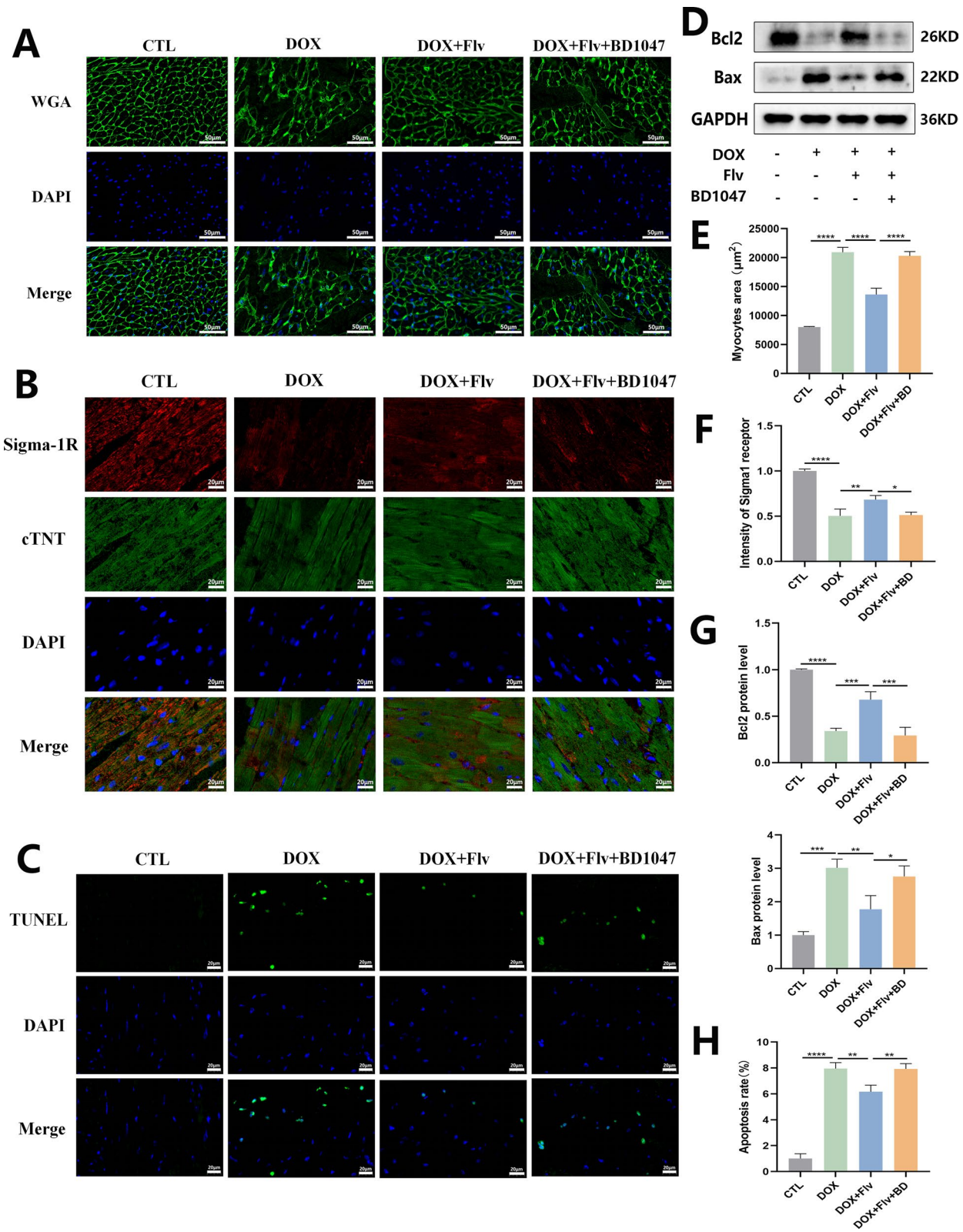

Fig. 3 (See legend on previous page.)

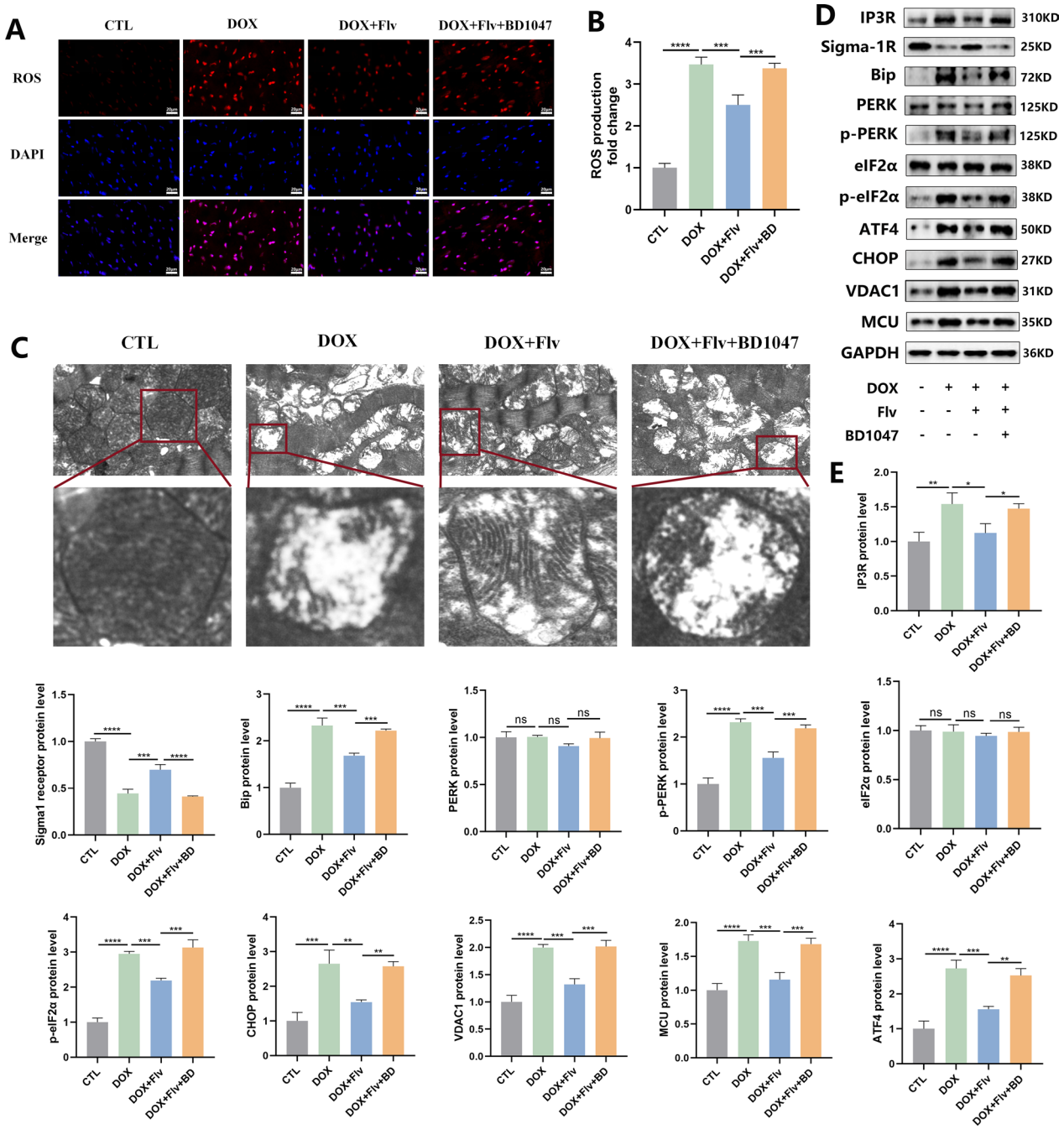

Fig. 4 Activation of S1R attenuates oxidative stress levels and mitigates mitochondrial damage in mouse heart. **A**, **B** DHE showed that activation of S1R attenuated ROS production in myocardial tissue (n = 3). **C** TEM detection showed activation of S1R improved mitochondrial morphology and attenuated mitochondrial injury. **D**, **E** Activation of S1R inhibited PERK and IP3R-VDAC1-MCU signaling pathways and alleviated endoplasmic reticulum stress and mitochondrial damage (n = 3). *:p < 0.05; **p < 0.01; ***p < 0.005; ****p < 0.001

Decreasing intracellular calcium levels in vitro reduces cardiomyocyte apoptosis

Evidence indicates that DOX triggers dysregulation of intracellular calcium homeostasis and ER stress. The ER is an intracellular calcium reservoir, and the MAM-located S1R receptor regulates calcium channels. We hypothesized that S1R exerts cardioprotection by attenuating the mitochondrial calcium overload and reducing calcium transport along the MAM network. Thus, we used BAPTA-AM, a calcium chelator, for our

in vitro experiments to further investigate the mechanism of S1R-exerted cardioprotective effects.

Calcium chelator BAPTA-AM crosses the cell membrane to reduce intracellular Ca^{2+} levels. We used an ER-tracker fluorochrome with S1R immunofluorescence co-localization to examine the receptor's expression and localization. We found that S1R has a broad distribution in the MAM network and connects closely with the ER. After stimulating cardiomyocytes with BAPTA-AM, S1R expression was unaffected but reduced significantly after BD1047 treatment (Fig. 6E, G). Next, we performed AO staining to detect apoptosis and uncovered that apoptotic cells (distinguished as bright yellow crumples) significantly reduced in the DOX + BAPTA-AM group compared with the DOX group. While more apoptotic cells were discovered after BD1047-induced S1R inhibition, their numbers again decreased when BAPTA-AM was applied with BD1047 (Fig. 6A–D). The AO staining observations were confirmed by quantifying apoptotic protein levels under the same treatment conditions using Western blotting. In conclusion, these findings suggest that the anti-apoptotic effect of S1R is related to the regulation of intracellular calcium homeostasis.

Lowering intracellular calcium levels in vitro relieves ER stress and reduces ER-mitochondrial contact

We examined S1R and IP3R expression using S1R and IP3R immunofluorescence double-labeling techniques. Cells in the DOX + BAPTA-AM group showed significantly reduced IP3R expression versus those in the DOX group (Fig. 6H, F). In addition, Western Blotting techniques showed that the PERK signaling pathway and VDAC1-MCU calcium transporter complex expression were significantly inhibited in DOX + BAPTA-AM-stimulated cells. By contrast, cells in the DOX + BD1047 group exhibited increased IP3R expression and an activated ER stress-related (PERK) signaling pathway versus those in the DOX group (Fig. 6I, J). Moreover, BD1047 counteracted the alleviating effect of BAPTA-AM in cells exposed to combined BD1047 and BAPTA-AM stimulation.

Subsequently, we investigated ROS production in mitochondria using a MitoSOX fluorescent probe for live cell imaging. Compared with cells in the DOX group, mitochondrial ROS production in cells in the DOX + BAPTA-AM group significantly dropped but rose after BD1047-induced S1R inhibition (Fig. 7A, B). We also detected the mitochondrial membrane potential using a JC-1 fluorescent probe. Whereas the cellular mitochondrial membrane potential was restored in the DOX + BAPTA-AM group, it decreased after BD1047-induced S1R inhibition, indicating that the inhibited receptor further aggravates mitochondrial damage. Conversely, BD1047 counteracted the protective effect of the calcium chelator on mitochondria in cells of the BD1047 + BAPTA-AM group (Fig. 7C, D).

Because calcium overload may provoke mitochondrial damage during DOX-induced cardiotoxicity, we used a Rhod-2 AM calcium fluorescent probe to assess intracellular Ca^{2+} levels. When cells were stimulated with BAPTA-AM, the intracellular Ca^{2+} concentration decreased significantly. By contrast, inhibiting S1R with BD1047 exacerbated ER stress and increased intracellular Ca^{2+} levels. Notably, Ca^{2+} levels were unaffected when cells were exposed to combined BAPTA-AM and BD1047 treatment (Fig. 7G, H). Mitochondrial fusion and fission also play a significant role in calcium overload and oxidative stress. Mitochondrial fusion helps alleviate mitochondrial oxidative stress and calcium overload, enhances beneficial mitophagy, and maintains the stability of MAM; conversely, excessive mitochondrial fission aggravates organelle damage, disrupts MAM, and intensifies calcium overload [30, 31]. The results of Western blotting (WB) indicated that after adding BAPTA-AM to chelate Ca^{2+}, the expression of Mfn2, an indicator of mitochondrial fusion, increased. In contrast, after adding BD1047 to inhibit S1R, the expression of Drp1, an indicator of mitochondrial fission, increased, and mitochondrial damage worsened (Fig. 7E, F). These findings confirm our conjecture that S1R relieves ER stress, which reduces Ca^{2+} release from the ER and Ca^{2+} transport to mitochondria and alleviates mitochondrial calcium overload, serving as a cell-preserving effect.

Finally, we used TEM to observe the ultrastructure of primary cardiomyocytes and elucidate the mechanism of S1R in the ER and mitochondria. We discovered that

(See figure on next page.)

Fig. 5 Activation of S1R attenuates cellular oxidative stress levels and reduces apoptosis in vitro. **A** Schematic protocol for Flv, BD1047, DOX, siRNA and BAPTA-AM treatment in vitro. **B** Apoptosis measurement by flow cytometry showed that activation of S1R reduced apoptosis. **C** Western blot showed activation of S1R reduced cardiomyocyte apoptosis. **D** The statistical analysis diagrams of apoptosis rate (n = 3). **E** The statistical analysis diagrams of Bcl2, Bax protein level relative to GAPDH (n = 3). **F**, **G** DCFH showed that stimulation of S1R reduced ROS production in cardiomyocytes (n = 3). **H** Immunofluorescence results showed decreased expression of S1R in cells given DOX. **I** Activation of S1R inhibited PERK and IP3R-VDAC1-MCU signaling pathways and alleviated endoplasmic reticulum stress and mitochondrial damage (n = 3). **J** The statistical analysis diagrams of immunofluorescence staining reflecting S1R expression (n = 3). **K** The statistical analysis diagrams of IP3R, S1R, Bip, PERK, p-PERK, eIF2α, p-eIF2α, ATF4, VDAC1, and MCU protein expression relative to GAPDH in cardiomyocyte (n = 3). *p < 0.05; **p < 0.01; ***p < 0.005; ****p < 0.001

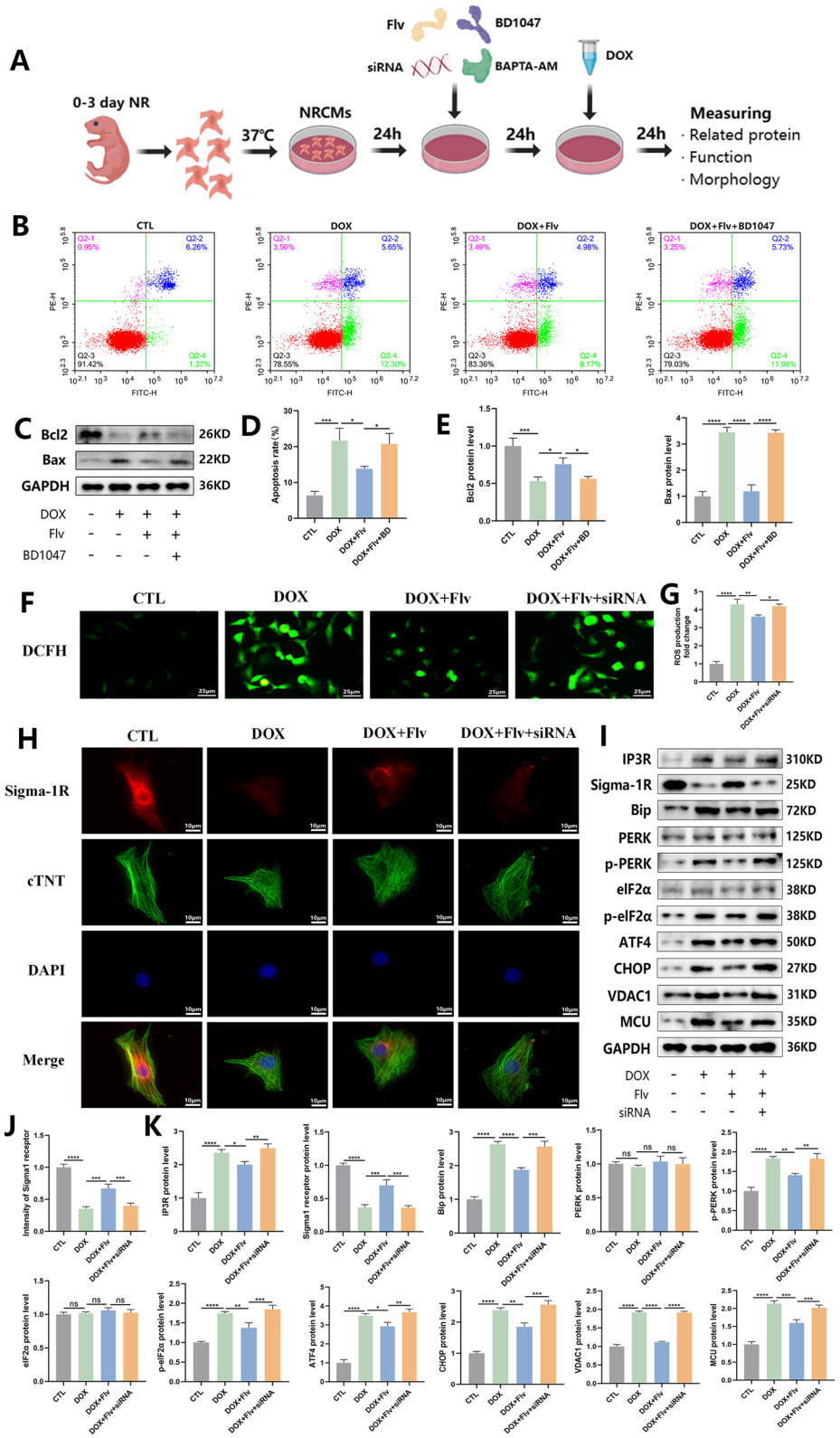

Fig. 5 (See legend on previous page.)

S1R, as a chaperone protein in the MAM network, effectively regulated the contact and distance between the ER and mitochondria. When cells suffered injury, the ER initiated a rapid stress response that prompted S1R dissociation from IP3R, reinforcing the contact between the ER and mitochondria and reducing the distance between the 2 organelles. By contrast, Flv-induced S1R activation and calcium-chelating agents effectively reduced the contact between mitochondria and the ER and increased the distance between them. In summary, our ultrastructure analysis suggests that the mechanism by which S1R exerts cardioprotective effects entails attenuating ER stress and reducing the contact between the ER and mitochondria, which in part works by diminishing mitochondrial calcium overload and regulating intracellular calcium levels (Fig. 7G, H).

Discussion

In this study, we demonstrated that the activated sigma-1 receptor effectively inhibits PERK and IP3R-VDAC1-MCU signaling pathways, attenuates ER stress, reduces the contact between the ER and mitochondria, and alleviates mitochondrial calcium overload. These events improve cardiac function, counteract DOX-induced cardiotoxicity, and delay its progression. Therefore, we propose that S1R is a potential therapeutic target for preventing and treating DOX-induced cardiotoxicity (Fig. 8).

Doxorubicin belongs to the family of anthracycline antibiotics, and its pharmacological action lies in the embedded interaction with human DNA [32]. As a result, it blocks tumor cell proliferation and induces apoptosis, making it a common broad-spectrum antitumor drug used in the clinic [33]. This drug has a therapeutic effect on various malignant tumors, including breast cancer, lymphoma, sarcoma, and certain types of leukemia [34]. Although an effective drug, it induces cardiotoxicity and attacks healthy heart muscle cells, limiting its clinical use. Recent studies have made progress in identifying the molecular targets and signaling pathways involved in DOX-induced cardiotoxicity and myocardial injury [24, 35, 36]. However, its clinical pharmacological approach is still poorly understood, and the mechanism by which it provokes cardiotoxicity has been a hot topic in oncology therapy.

Endoplasmic reticulum stress has been proposed as an integral part of the mechanism of DOX-induced cardiotoxicity [37]. The ER is a vital organelle responsible for protein synthesis and Ca^{2+} storage, which is necessary for cardiac contractions [38]. When unfolded or misfolded proteins accumulate in the ER in response to an external stimulus, the ER initiates a stress program for self-protection [39]. Numerous VDAC-MCU calcium channel transporter complexes are activated and release excess Ca^{2+} ions into the cytoplasm and mitochondria, where they accumulate, triggering mitochondrial calcium overload [40]. Prolonged ER stress affects the ATP-generating electron transport chain through the mitochondrial pathway, inducing cell necrosis and apoptosis in the heart [41]. The width of the MAM is recognized as a parameter that tightly regulates its function and calcium channels [42]. The sigma-1 receptor is a vital ER transmembrane protein with a key role in the signaling crosstalk across the MAM network [43, 44]. In healthy cells, S1R localizes in ER lipid rafts and forms a complex with the BiP chaperone attached to the luminal side of IP3R, maintaining IP3R structure and function stability [43, 45]. Under normal physiological stimuli, such as ATP stimulation of normal intensity, the S1R-IP3R-BiP complex is localized in the MAM in a dormant state [46]. However, under sustained external high-intensity stimulation, S1R dissociates from IP3R and redistributes to the entire ER membrane to evoke a protective effect on the cell [47]. Thus, inhibiting ER stress via S1R activation may be a new target for alleviating cardiotoxicity.

The MAM is a reticular structure between mitochondria and the ER and forms a pivotal bridge connecting the two organelles. S1R is responsible for maintaining the dynamic balance between the amount of MAM and the interface structure [48]. Under pathological conditions, such as diabetes, cardiotoxicity, and neurodegenerative

(See figure on next page.)

Fig. 6 Calcium chelator BAPTA-AM attenuates cardiomyocyte apoptosis and reduces endoplasmic reticulum stress. **A** AO staining showed that BAPTA-AM reduced apoptosis, however, apoptosis increased after inhibition of S1R. **B** Western blot showed that BAPTA-AM decreased apoptosis, while inhibition of S1R increased apoptosis. **C** The statistical analysis diagrams of apoptotic cell percentage (n = 3). **D** The statistical analysis diagrams of Bcl2, Bax protein level relative to GAPDH (n = 3). **E** The statistical analysis diagrams of immunofluorescence staining reflecting S1R expression (n = 3). **F** The statistical analysis diagrams of immunofluorescence staining reflecting S1R and IP3R expression (n = 3). **G** Immunofluorescence showed that the endoplasmic reticulum was tightly connected to the S1R and the addition of BAPTA-AM did not affect the expression of the S1R. **H** Immunofluorescence showed a decrease in intracellular IP3R expression after addition of BAPTA-AM, and conversely, an increase in IP3R expression after inhibition of the S1R. **I** Western blot showed addition of BAPTA-AM inhibited PERK and IP3R-VDAC1-MCU signaling pathways and alleviated endoplasmic reticulum stress and mitochondrial damage. **J** The statistical analysis diagrams of IP3R, S1R, Bip, PERK, p-PERK, eIF2α, p-eIF2α, ATF4, VDAC1, and MCU protein expression relative to GAPDH in cardiomyocyte (n = 3). $^{**}p < 0.01$; $^{***}p < 0.005$; $^{****}p < 0.001$

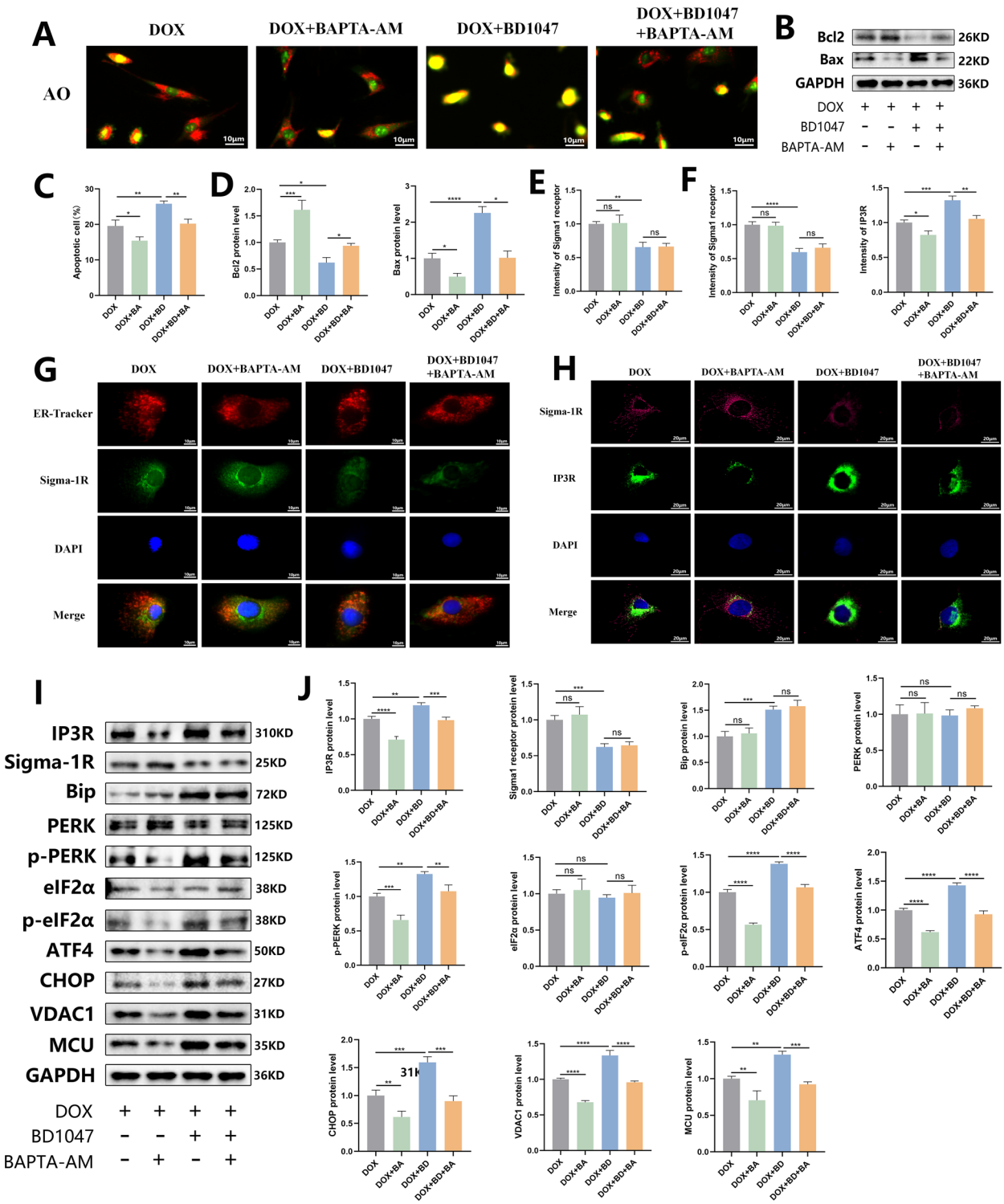

Fig. 6 (See legend on previous page.)

diseases, the ER triggers a stress response that induces conformational changes in the MAM, reducing the distance between the ER and mitochondria and increasing their contact [49]. The resulting mitochondrial calcium overload impairs the mitochondrial structure and function, driving cell necrosis and apoptosis [50]. Evidence

shows that S1R knockout mice exhibit MAM deficiency [27], reinforcing that S1R is an essential protein in MAM regulation. Our study also confirmed this observation since our TEM results showed that Flv-induced S1R activation increases the distance between mitochondria and the ER and decreases their contact. As a result, we noticed fewer calcium transporter complexes and a partially restored mitochondrial membrane potential. Conversely, BD1047-triggered S1R inhibition increased the contact between the ER and mitochondria, promoted calcium transporter complexes, and enhanced intracellular Ca^{2+} levels. The intracellular Ca^{2+} surge and the consequential calcium overload in mitochondria worsened mitochondrial oxidative stress, damaging mitochondrial structure and negatively affecting cell survival and function.

The PERK signaling pathway is one of the several signaling pathways that initiate ER stress in the cell [51]. The PERK protein is a stress-sensitive ER transmembrane kinase with a serine/threonine cytoplasmic structural domain. Various molecular chaperones (e.g., GRP78/BiP) maintain the kinase activity of the PERK luminal structural domain in an inactive state [52]. Under ER stress, GRP78/BiP proteins dissociate from PERK, causing homo-oligomerization of the PERK structural domain. The released PERK is activated by oligomerization and reverse autophosphorylation, and the activated PERK phosphorylates the alpha subunit of translation initiation factor 2 (eIF-2α) [53]. In the early stages of the stress response, phosphorylated eIF2α inhibits protein translation and synthesis, reducing the load of protein folding in the ER and exerting a protective effect on the cells [54]. As the stress response intensifies, phosphorylated eIF-2α induces the expression of the ATF4 transcription factor, promoting the expression of C/EBP homologous protein (CHOP) and cell apoptosis [55]. In addition, PERK can also interact with S1R to form a PERK-S1R complex, jointly stabilizing the structure of MAM [18]. When Flv is used to activate S1R, the binding between PERK and S1R becomes tighter, the dissociation of PERK from the complex decreases, and the downstream phosphorylation process is blocked, thereby inhibiting the PERK pathway. Our research has also verified this process. After activating S1R, the PERK pathway is inhibited, and the expression of downstream indicators all decreases. Conversely, when S1R is inhibited by BD1047, the PERK pathway is activated, and endoplasmic reticulum stress is exacerbated. Given these points, we conclude that activated S1R is a central target to regulate the ER stress pathway during DOX-induced [56] myocardial injury.

Limitations

Although our study offers valuable and novel insights into the mechanism underlying the cardioprotective effect of S1R in doxorubicin-induced cardiotoxicity, it still has several limitations. Firstly, S1R is prevalently present in the central nervous system and peripheral organs, such as the heart and liver. Since we activated or inhibited S1R by administering relevant drugs through intraperitoneal injection, the possibility that the central nervous system modulates the structural and functional aspects of the heart and cardiomyocytes via the brain–heart axis cannot be ruled out. Furthermore, we determined mitochondrial function by observing the ultrastructure of cells using transmission electron microscopy, without quantitatively measuring respiratory oxygen consumption and ATP production. Finally, we employed 8-week-old mice in the experiment, but most patients who develop cardiotoxicity due to the use of DOX in the clinical setting are elderly. Whether the use of aged mice for research is necessary awaits further exploration and validation. Therefore, these issues should be addressed in future investigations to confirm the results presented in our study.

Conclusion

Activating the sigma-1 receptor evokes a cardioprotective effect on the heart that alleviates DOX-induced cardiotoxicity. The activated receptor modulates ER-mitochondrial contact, alleviates ER stress, reduces mitochondrial calcium overload, decreases ROS production, and improves cardiac function. This sigma-1-promoted

(See figure on next page.)

Fig. 7 S1R can improve endoplasmic reticulum and mitochondrial function by regulating MAM and Ca^{2+} concentrations. **A**, **B** MitoSOX showed that BAPTA-AM mitigates mitochondrial ROS production, whereas inhibition of S1R increased mitochondrial oxidative stress (n = 3). **C**, **D** JC-1 staining showed that inhibition of S1R decreased mitochondrial membrane potential and aggravated mitochondrial damage, whereas BAPTA-AM could restore mitochondrial membrane potential to some extent (n = 3). **E** Western blot showed that the addition of BAPTA-AM increased mitochondrial fusion, while the addition of S1R inhibitor BD1047 promoted mitochondrial fission. **F** The statistical analysis diagrams of Mfn2 and Drp1 protein expression relative to GAPDH in cardiomyocyte (n = 3). **G**, **H** Ca^{2+} fluorescence staining showed that inhibition of S1R increased intracellular calcium concentration, whereas the use of BAPTA-AM was effective in decreasing it (n = 3). **I** The statistical analysis diagrams of ER-mitochondrian distance (n = 3). **J** TEM showed that activation of S1R modulates MAM and increased the distance between the endoplasmic reticulum one and mitochondria, whereas inhibition of S1R enhanced mitochondrial and endoplasmic reticulum contacts. $^{**}p < 0.01$; $^{***}p < 0.005$; $^{****}p < 0.001$

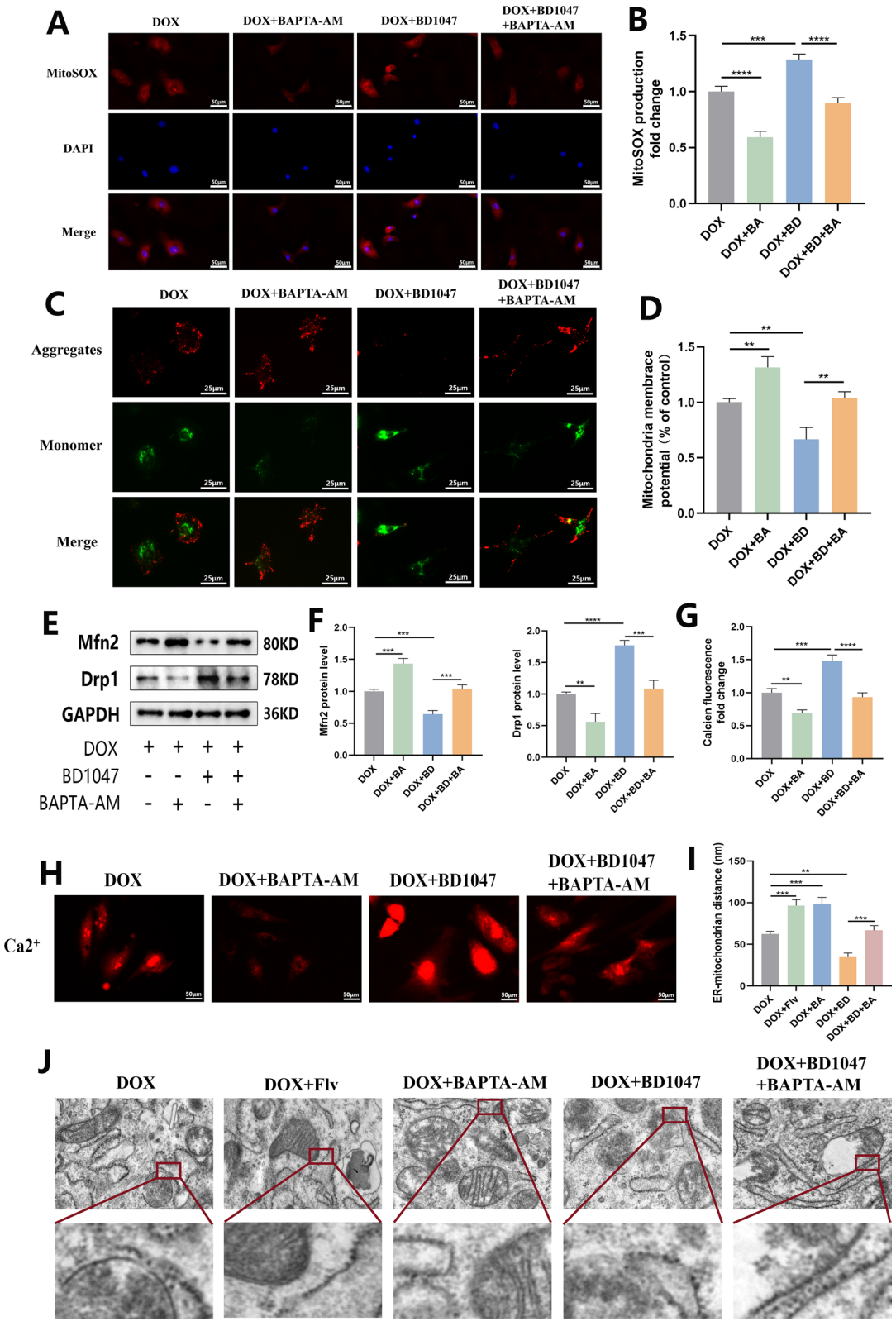

Fig. 7 (See legend on previous page.)

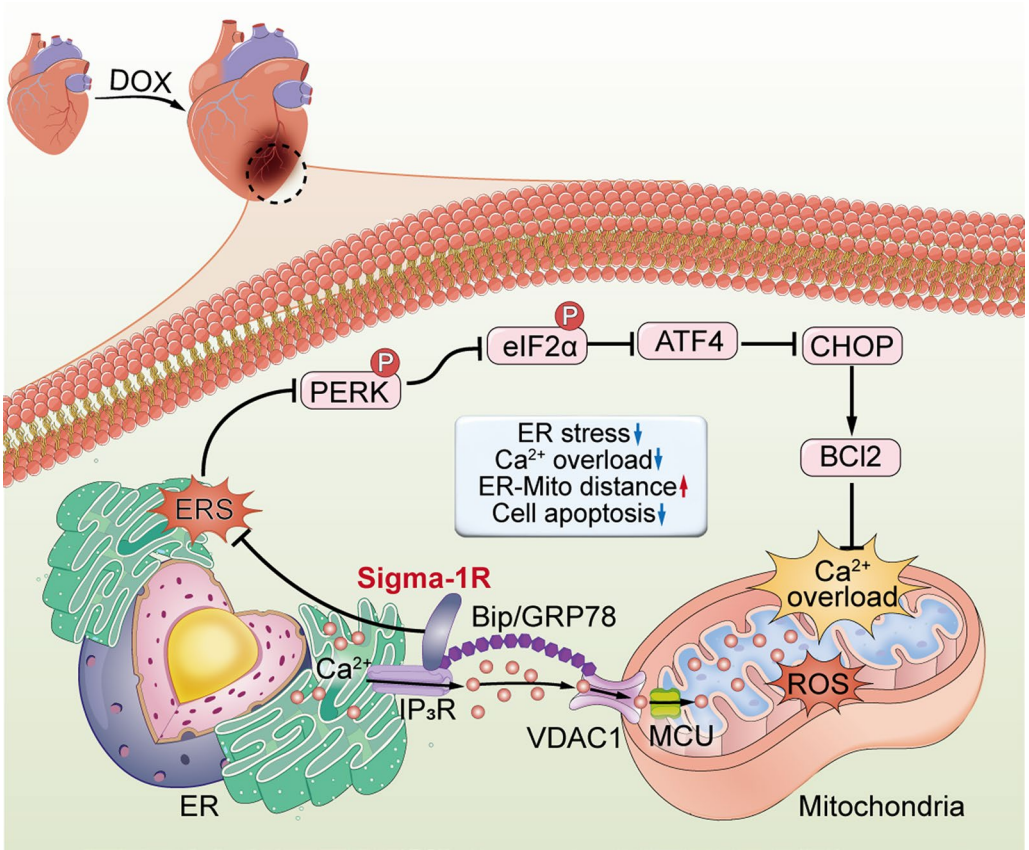

Fig. 8 Schematic representation on activation of S1R to modulate MAM and ameliorate endoplasmic reticulum stress and mitochondrial calcium overload. S1R exerts cardioprotective effects through PERK and IP3R-VDAC1-MCU signaling pathways

cardioprotective effect is achieved via PERK and IP3R-VDAC1-MCU signaling pathways.

Author contributions

ZXL, QR, CQ and BY designed this research; ZXL, CQ, SH, SYC and performed the experiments; ZXL and QR analyzed and interpreted the results; ZXL drafted manuscript; ZXL, QR and CQ revised the manuscript; BY and BS determined the final version of manuscript. All authors read and approved the final manuscript.

Funding

This study was supported by the National Natural Science Foundation of China (No. 82170316).

Availability of data and materials

The datasets used and/or analyzed during the current study are available from the corresponding author on reasonable request.

Declarations

Ethics approval and consent to participate

All protocols of animal experiments were approved by the Animal Experiment Ethics Committee of Wuhan Myhalic Biotechnology. All experiments were officially permitted and performed in Hubei Key Laboratory of Cardiology, complied with the Guide for the Care and Use of Laboratory Animals published by the US National Institutes of Health.

Consent for publication

Not applicable.

Competing interests

The authors declare that they have no competing interest.

Author details

[1]Department of Cardiology, Renmin Hospital of Wuhan University, 238 Jiefang Road, Wuhan 430060, China. [2]Cardiovascular Research Institute, Wuhan University, Wuhan 430060, China. [3]Hubei Key Laboratory of Cardiology, Wuhan 430060, China. [4]Department of Cardiology, the Central Hospital of Wuhan, Tongji Medical College, Huazhong University of Science and Technology, Wuhan 430014, China.

Received: 30 October 2024 Accepted: 12 February 2025
Published online: 25 February 2025

References

1. Aloss K, Hamar P. Recent preclinical and clinical progress in liposomal doxorubicin. Pharmaceutics. 2023;15(3):893.
2. Gambardella J, Santulli G, Fiordelisi A, et al. Infiltrating macrophages amplify doxorubicin-induced cardiac damage: role of catecholamines. Cell Mol Life Sci. 2023;80(11):323.
3. Wang AJ, Zhang J, Xiao M, et al. Molecular mechanisms of doxorubicin-induced cardiotoxicity: novel roles of sirtuin 1-mediated signaling pathways. Cell Mol Life Sci. 2021;78(7):3105–25.

4. Li X. Doxorubicin-mediated cardiac dysfunction: revisiting molecular interactions, pharmacological compounds and (nano)theranostic platforms. Environ Res. 2023;234: 116504.
5. Chen R, Niu M, Hu X, et al. Targeting mitochondrial dynamics proteins for the treatment of doxorubicin-induced cardiotoxicity. Front Mol Biosci. 2023;10:1241225.
6. Wu L, Wang L, Du Y, et al. Mitochondrial quality control mechanisms as therapeutic targets in doxorubicin-induced cardiotoxicity. Trends Pharmacol Sci. 2023;44(1):34–49.
7. Hayashi T, Rizzuto R, Hajnoczky G, et al. MAM: more than just a housekeeper. Trends Cell Biol. 2009;19(2):81–8.
8. Chakraborty J, Caicci F, Roy M, et al. Investigating mitochondrial autophagy by routine transmission electron microscopy: seeing is believing? Pharmacol Res. 2020;160: 105097.
9. Berridge MJ. The inositol trisphosphate/calcium signaling pathway in health and disease. Physiol Rev. 2016;96(4):1261–96.
10. Boyman L, Karbowski M, Lederer WJ. Regulation of mitochondrial ATP production: Ca(2+) signaling and quality control. Trends Mol Med. 2020;26(1):21–39.
11. Combot Y, Salo VT, Chadeuf G, et al. Seipin localizes at endoplasmic-reticulum-mitochondria contact sites to control mitochondrial calcium import and metabolism in adipocytes. Cell Rep. 2022;38(2): 110213.
12. Kumar V, Maity S. ER stress-sensor proteins and ER-mitochondrial cross-talk-signaling beyond (ER) stress response. Biomolecules. 2021;11(2):173.
13. Ehmke H. The sigma-1 receptor: a molecular chaperone for the heart and the soul? Cardiovasc Res. 2012;93(1):6–7.
14. Hashimoto K. Sigma-1 receptor chaperone and brain-derived neurotrophic factor: emerging links between cardiovascular disease and depression. Prog Neurobiol. 2013;100:15–29.
15. Zhao X, Liu X, Chen X, et al. Activation of the sigma-1 receptor exerts cardioprotection in a rodent model of chronic heart failure by stimulation of angiogenesis. Mol Med. 2022;28(1):87.
16. Bhuiyan MS, Fukunaga K. Targeting sigma-1 receptor signaling by endogenous ligands for cardioprotection. Expert Opin Ther Targets. 2011;15(2):145–55.
17. Omi T, Tanimukai H, Kanayama D, et al. Fluvoxamine alleviates ER stress via induction of Sigma-1 receptor. Cell Death Dis. 2014;5(7): e1332.
18. Mao H, Chen W, Chen L, et al. Potential role of mitochondria-associated endoplasmic reticulum membrane proteins in diseases. Biochem Pharmacol. 2022;199: 115011.
19. Hu C, Zhang X, Wei W, et al. Matrine attenuates oxidative stress and cardiomyocyte apoptosis in doxorubicin-induced cardiotoxicity via maintaining AMPKα/UCP2 pathway. Acta Pharm Sin B. 2019;9(4):690–701.
20. Zhang X, Hu C, Kong CY, et al. FNDC5 alleviates oxidative stress and cardiomyocyte apoptosis in doxorubicin-induced cardiotoxicity via activating AKT. Cell Death Differ. 2020;27(2):540–55.
21. Tagashira H, Bhuiyan S, Shioda N, et al. Sigma1-receptor stimulation with fluvoxamine ameliorates transverse aortic constriction-induced myocardial hypertrophy and dysfunction in mice. Am J Physiol Heart Circ Physiol. 2010;299(5):H1535–45.
22. Tagashira H, Bhuiyan MS, Shioda N, et al. Fluvoxamine rescues mitochondrial Ca^{2+} transport and ATP production through σ(1)-receptor in hypertrophic cardiomyocytes. Life Sci. 2014;95(2):89–100.
23. Liu DY, Chi TY, Ji XF, et al. Sigma-1 receptor activation alleviates blood–brain barrier dysfunction in vascular dementia mice. Exp Neurol. 2018;308:90–9.
24. Hu C, Zhang X, Song P, et al. Meteorin-like protein attenuates doxorubicin-induced cardiotoxicity via activating cAMP/PKA/SIRT1 pathway. Redox Biol. 2020;37: 101747.
25. Qu J, Li M, Li D, et al. Stimulation of sigma-1 receptor protects against cardiac fibrosis by alleviating IRE1 pathway and autophagy impairment. Oxid Med Cell Longev. 2021;2021:8836818.
26. Duran J, Troncoso MF, Lagos D, et al. GDF11 modulates Ca(2+)-dependent Smad2/3 signaling to prevent cardiomyocyte hypertrophy. Int J Mol Sci. 2018;19(5):1508.
27. Luo L, Ning F, Du Y, et al. Calcium-dependent Nedd4–2 upregulation mediates degradation of the cardiac sodium channel Nav1.5: implications for heart failure. Acta Physiol (Oxf). 2017;221(1):44–58.
28. Peng YS, Ding HC, Lin YT, et al. Uremic toxin p-cresol induces disassembly of gap junctions of cardiomyocytes. Toxicology. 2012;302(1):11–7.
29. Vahabzadeh G, Soltani H, Barati M, et al. Noscapine protects the H9c2 cardiomyocytes of rats against oxygen-glucose deprivation/reperfusion injury. Mol Biol Rep. 2020;47(8):5711–9.
30. Jiang Y, Krantz S, Qin X, et al. Caveolin-1 controls mitochondrial damage and ROS production by regulating fission–fusion dynamics and mitophagy. Redox Biol. 2022;52: 102304.
31. Chen H, Detmer SA, Ewald AJ, et al. Mitofusins Mfn1 and Mfn2 coordinately regulate mitochondrial fusion and are essential for embryonic development. J Cell Biol. 2003;160(2):189–200.
32. Launchbury AP, Habboubi N. Epirubicin and doxorubicin: a comparison of their characteristics, therapeutic activity and toxicity. Cancer Treat Rev. 1993;19(3):197–228.
33. Almajidi YQ, Kadhim MM, Alsaikhan F, et al. Doxorubicin-loaded micelles in tumor cell-specific chemotherapy. Environ Res. 2023;227: 115722.
34. He F, Xie C, Xu X. Hyaluronic acid-modified yeast β-glucan particles delivering doxorubicin for treatment of breast cancer. Carbohydr Polym. 2023;314: 120907.
35. Qiao X, van der Zanden SY, Wander DPA, et al. Uncoupling DNA damage from chromatin damage to detoxify doxorubicin. Proc Natl Acad Sci USA. 2020;117(26):15182–92.
36. Jiang Q, Chen X, Tian X, et al. Tanshinone I inhibits doxorubicin-induced cardiotoxicity by regulating Nrf2 signaling pathway. Phytomedicine. 2022;106: 154439.
37. Nakagama S, Maejima Y, Fan Q, et al. Endoplasmic reticulum selective autophagy alleviates anthracycline-induced cardiotoxicity. JACC CardioOncol. 2023;5(5):656–70.
38. Ron D, Walter P. Signal integration in the endoplasmic reticulum unfolded protein response. Nat Rev Mol Cell Biol. 2007;8(7):519–29.
39. Schwarz DS, Blower MD. The endoplasmic reticulum: structure, function and response to cellular signaling. Cell Mol Life Sci. 2016;73(1):79–94.
40. Roca FJ, Whitworth LJ, Redmond S, et al. TNF induces pathogenic programmed macrophage necrosis in tuberculosis through a mitochondrial-lysosomal-endoplasmic reticulum circuit. Cell. 2019;178(6):1344-61.e11.
41. Arruda AP, Pers BM, Parlakgül G, et al. Chronic enrichment of hepatic endoplasmic reticulum-mitochondria contact leads to mitochondrial dysfunction in obesity. Nat Med. 2014;20(12):1427–35.
42. Cho E, Woo Y, Suh Y, et al. Ratiometric measurement of MAM Ca(2+) dynamics using a modified CalfluxVTN. Nat Commun. 2023;14(1):3586.
43. Hayashi T, Su TP. Sigma-1 receptor chaperones at the ER-mitochondrion interface regulate Ca(2+) signaling and cell survival. Cell. 2007;131(3):596–610.
44. Zhou Z, Torres M, Sha H, et al. Endoplasmic reticulum-associated degradation regulates mitochondrial dynamics in brown adipocytes. Science. 2020;368(6486):54–60.
45. Maurice T, Su TP. The pharmacology of sigma-1 receptors. Pharmacol Ther. 2009;124(2):195–206.
46. Couly S, Yasui Y, Su TP. SIGMAR1 confers innate resilience against neurodegeneration. Int J Mol Sci. 2023;24(9):7767.
47. Hayashi T, Su TP. Regulating ankyrin dynamics: roles of sigma-1 receptors. Proc Natl Acad Sci USA. 2001;98(2):491–6.
48. Crouzier L, Danese A, Yasui Y, et al. Activation of the sigma-1 receptor chaperone alleviates symptoms of Wolfram syndrome in preclinical models. Sci Transl Med. 2022;14(631):eabh3763.
49. Hu Y, Chen H, Zhang L, et al. The AMPK-MFN2 axis regulates MAM dynamics and autophagy induced by energy stresses. Autophagy. 2021;17(5):1142–56.
50. Cao X, Chen Y. Mitochondria and calcium signaling in embryonic development. Semin Cell Dev Biol. 2009;20(3):337–45.
51. Mandula JK, Chang S, Mohamed E, et al. Ablation of the endoplasmic reticulum stress kinase PERK induces paraptosis and type I interferon to promote anti-tumor T cell responses. Cancer Cell. 2022;40(10):1145-60.e9.
52. Bettigole SE, Glimcher LH. Endoplasmic reticulum stress in immunity. Annu Rev Immunol. 2015;33:107–38.
53. Almeida LM, Pinho BR, Duchen MR, et al. The PERKs of mitochondria protection during stress: insights for PERK modulation in neurodegenerative and metabolic diseases. Biol Rev Camb Philos Soc. 2022;97(5):1737–48.
54. Verfaillie T, Rubio N, Garg AD, et al. PERK is required at the ER-mitochondrial contact sites to convey apoptosis after ROS-based ER stress. Cell Death Differ. 2012;19(11):1880–91.

55. Xu S, Xu Y, Chen L, et al. RCN1 suppresses ER stress-induced apoptosis via calcium homeostasis and PERK-CHOP signaling. Oncogenesis. 2017;6(3):e304.
56. Balsa E, Soustek MS, Thomas A, et al. ER and nutrient stress promote assembly of respiratory chain supercomplexes through the PERK-eIF2α axis. Mol Cell. 2019;74(5):877–90.e6.

Publisher's Note